Plant Pathology

WILEY

ORIGINAL ARTICLE OPEN ACCESS

Genetic Characterisation and Aggressiveness of the *Fusarium oxysporum* Species Complex in Tomato Plants and Irrigation Water From Australian Processing Fields

Hanyue Feng[1] | Sophia E. Callaghan[2] | Jiajing Cao[1] | Paul W. J. Taylor[1] | Sigfredo Fuentes[1] | Alexis Pang[1] | Yu Pei Tan[3,4] | Niloofar Vaghefi[1,3]

[1]School of Agriculture, Food and Ecosystem Sciences, Faculty of Science, The University of Melbourne, Parkville, Victoria, Australia | [2]Department of Agriculture, Fisheries and Forestry, Mascot, New South Wales, Australia | [3]Centre for Crop Health, University of Southern Queensland, Toowoomba, Queensland, Australia | [4]Queensland Department of Primary Industries, Dutton Park, Queensland, Australia

Correspondence: Niloofar Vaghefi (vaghefin@unimelb.edu.au)

Received: 11 November 2025 | **Revised:** 2 March 2026 | **Accepted:** 20 July 2026

Keywords: epidemiology | genetic diversity | pathogenicity | phylogeny | soilborne pathogens | yield decline

ABSTRACT

Fusarium oxysporum Species Complex (FOSC) includes important soil-borne pathogens of a range of crops worldwide. In Victoria and New South Wales, Australia, FOSC has been identified as the cause of stunting and poor growth in processing tomato fields, resulting in significant yield losses. A total of 40 FOSC isolates were obtained from symptomatic tomato plants, irrigation water samples and culture collections, which were confirmed to be FOSC by multigene phylogenetic analyses based on four genomic loci: β-tubulin, calmodulin, the second largest subunit of nuclear RNA polymerase II and translation elongation factor 1-α. There was a high level of genetic diversity among isolates, with multiple phylogenetic lineages detected. Glasshouse bioassays demonstrated that all tested isolates were pathogenic to processing tomato, resulting in significant reductions in plant growth, with above-ground height reduced by 11%–26% and root dry weight by 44%–83% compared with the control ($p < 0.05$). Although aggressiveness varied among isolates, growth reduction occurred irrespective of their phylogenetic placement. Moreover, the shared genetic background of isolates from irrigation water and plant samples highlights the role of irrigation water as a potential source of inoculum in *Fusarium* epidemics, underscoring its significance for disease management in Australian processing tomato systems.

1 | Introduction

Tomato is one of the most important vegetable crops globally, grown in variable climatic conditions and soil profiles (Zhu and Miller 2025). There are two major types of cultivated tomatoes: one for fresh consumption, for example salad tomato that is usually grown under controlled environments (Cammarano et al. 2022); and processing tomato used for canned products, ketchup and sauces that is mostly grown under field conditions (Ma et al. 2023). The major production areas of processing tomatoes include California, the United States (Swett et al. 2023), Italy (Caruso et al. 2022) and China (Yang et al. 2023).

In Australia, tomato is the second-most profitable vegetable commodity (McKenzie et al. 2017). In the 2022/23 growing season, 321,736 t of tomatoes were produced, valued at $570.6 million with 34% designated for the processing industry (Stewart 2023). Approximately 2000–3000 ha of processing tomatoes are produced annually, of which 75% is in northern Victoria (VIC) and the remaining 25% in New South Wales (NSW) (Ma et al. 2023). Over the past decade, an estimated 10% annual yield loss in Australian processing tomato production has been attributed to soil-borne diseases (Callaghan et al. 2018), with *Fusarium oxysporum* identified as a major contributing factor. Members of the *Fusarium oxysporum* Species Complex (FOSC) are among the

most destructive soil-borne pathogens affecting tomato crops worldwide (Ramsey et al. 1992; Swett et al. 2023). While *F. oxysporum* is well known for its persistence in soil, recent studies suggest that irrigation water may also serve as a potential source of FOSC inoculum, particularly with the increasing use of recycled or surface water in agricultural systems (McGovern 2015). This highlights the importance of considering both soil- and water-borne pathways in the epidemiology and management of *F. oxysporum* in processing tomato production.

In recent years, extensive research on FOSC has led to recognition of numerous cryptic species based on a phylogenetic species concept, ranging from 3 to 15 species (Achari et al. 2020; Laurence et al. 2012; Lombard et al. 2019; O'Donnell et al. 1998). The molecular taxonomy of *F. oxysporum* has consequently undergone several revisions, with multiple frameworks proposed by different research groups. These efforts have been further complicated by evidence of horizontal gene transfer and genetic recombination within the complex (Zhang et al. 2020). Within FOSC, while isolates are traditionally grouped into *formae speciales* (f. sp.) based on host specificity (Lievens et al. 2008), these phenotypic classifications cannot be reliably inferred from phylogeny or effector gene profiles alone, as the definition of f. sp. is phenotypic, relying on the host range and differential pathogenicity assays rather than genetic relatedness (Baayen et al. 2000). Genetically similar isolates can, therefore, differ in pathogenicity and host interactions, and isolates assigned to the same f. sp. may fall into distinct phylogenetic clades (Afordoanyi et al. 2022). This highlights that understanding FOSC requires integrating both genetic and phenotypic analyses, with experimental assessment of pathogenicity remaining essential to characterise isolate diversity and impact.

Historically, O'Donnell et al. (1998) used translation elongation factor 1-α (*tef1-α*) and the mitochondrial small subunit of the ribosomal RNA genes (*mtSSU rDNA*) to test the monophyly of several *F. oxysporum* isolates. Their analyses revealed that although *F. oxysporum* formed a monophyletic clade, both pathogenic and nonpathogenic *F. oxysporum* isolates occurred within the same evolutionary lineages. Moreover, many *formae speciales*, including f. sp. *cubense* causing Panama disease on banana, and f. sp. *lycopersici* and *radicis-lycopersici* associated with tomato diseases, were polyphyletic, with several isolates having independent evolutionary origins. This suggested that host pathogenicity evolved convergently in *F. oxysporum*. Similarly, a later study by Laurence et al. (2012) used the same genes, *tef1-α* and *mtSSU rDNA*, to genetically characterise Australian *F. oxysporum* isolates collected from native ecosystems representing four different climatic conditions using the same dataset as proposed by O'Donnell et al. (1998). The Australian isolates were separated into five clades that indicated high genetic diversity (Laurence et al. 2012); however, host pathogenicity of the isolates was not assessed.

More recently, Lombard et al. (2019) used four genes: β-tubulin (*tub2*), calmodulin (*cmdA*), the second largest subunit of nuclear RNA polymerase II (*rpb2*) and *tef1-α* for multilocus phylogenetic inference. They combined this with morphological studies to resolve cryptic speciation within FOSC and described 15 separate species within eight major clades. Later, Achari et al. (2020) applied multispecies coalescent analyses to whole genomes, nuclear genes and mitochondrial genome sequence data to reconstruct the phylogeny of *F. oxysporum* isolates from both natural and agricultural ecosystems in Australia. Three major phylogenetic clades were consistently identified across all phylogenies, with two additional single-isolate clades. Therefore, it was suggested that the three clades may be considered as separate species, with Clade 3 representing *F. oxysporum sensu stricto* as it contained the neotype of *F. oxysporum*.

Secreted In Xylem (*SIX*) genes have been widely studied as key effectors contributing to virulence and host–pathogen interactions within the FOSC, particularly in well-characterised pathosystems such as *F. oxysporum* f. sp. *lycopersici* (Jangir et al. 2021). These genes, often located on lineage-specific or mobile pathogenicity chromosomes, can play important roles in determining compatibility with specific hosts and in triggering host resistance responses. However, increasing evidence indicates that the presence, absence or diversity of *SIX* genes does not consistently align with phylogenetic relationships or reliably delineate *formae speciales* across the FOSC (Afordoanyi et al. 2022). Recent work has highlighted that host specificity in *F. oxysporum* may be more flexible and context-dependent than previously assumed, with multiple genetic lineages capable of infecting the same host and individual *formae speciales* not representing discrete evolutionary units (Han et al. 2025). As a result, while *SIX* genes provide valuable insight into pathogenic mechanisms, they are not currently incorporated into taxonomic frameworks for FOSC. Accordingly, the present study focuses on multilocus phylogenetic analyses and pathogenicity assays to resolve taxonomic relationships among *F. oxysporum* isolates associated with processing tomato in Australia, rather than on effector profiling.

The phylogenetic placement of Australian *F. oxysporum* isolates recovered from processing tomato plants, along with their pathogenicity and aggressiveness toward local cultivars, remains poorly understood. To address this knowledge gap, our study aimed to (1) recover and genetically characterise *F. oxysporum* isolates associated with poor growth of processing tomatoes from affected fields in VIC and NSW, Australia; (2) investigate their phylogenetic relationships using different taxonomic frameworks; and (3) evaluate the pathogenicity and aggressiveness of representative isolates through replicated glasshouse bioassays. In this context, pathogenicity refers to the ability of an isolate to cause disease, whereas aggressiveness denotes the quantitative degree of disease severity expressed by a pathogenic isolate (De Silva et al. 2021).

2 | Materials and Methods

2.1 | Sample Collection and Pathogen Isolation

During the 2022, 2023 and 2024 growing seasons, a total of 28 symptomatic processing tomato plants were collected from 20 commercial fields in VIC and NSW, along with six irrigation water samples from one field in NSW. For plant sampling, whole tomato plants showing stunting, chlorosis and poor growth (Figure 1) were carefully uprooted and transported to the laboratory. Samples were stored at 5°C for a maximum of 48 h before fungal isolation. For irrigation water sampling, six samples

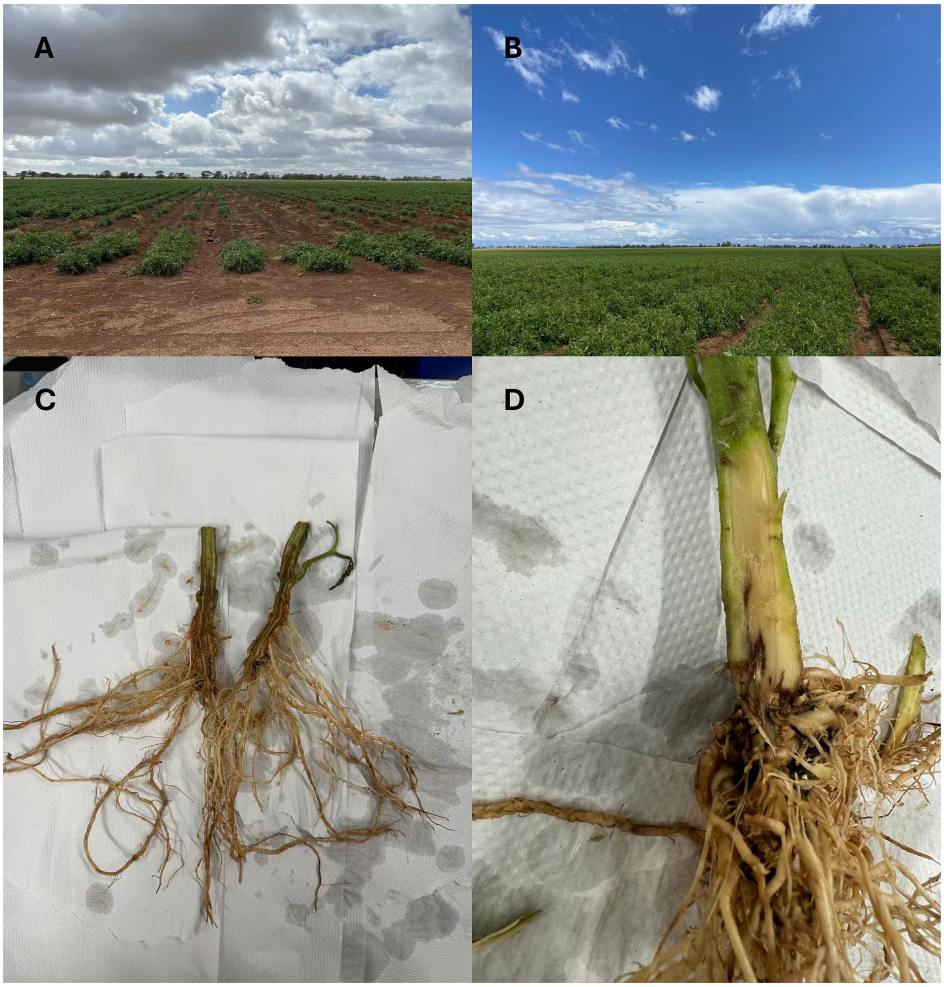

FIGURE 1 | Comparison of (A) a disease-affected field with severe patchiness with a (B) healthy processing tomato field. (C, D) Collar, root and shoot regions of *Fusarium oxysporum*-infected processing tomato plants, demonstrating poor root development and necrotic discolouration of the internal stem.

along five points of the irrigation system were collected; these included point 1: one sample from irrigation channel water as it entered the property; point 2: one sample from on-farm reservoir filled with water from irrigation channel; point 3: one sample from on-farm reservoir filled with rain and irrigation runoff; point 4: one sample from filtered water after leaving point 2 and before entering the irrigation system; and point 5: two water samples from irrigation drip lines in the field (Table 1).

For isolations from plant tissue, collected plants were gently washed under running tap water for approximately 5 min to remove adhering soil particles. From each plant, symptomatic sections (around 5 mm^2) were excised from the roots, collar and lower stem tissues whenever symptoms were present. In most cases, multiple tissues from the same plant were sampled to increase the likelihood of pathogen recovery, while in a few plants only one or two tissue types were available due to limited symptom development. Tissue pieces were surface-sterilised by immersion in 1% (active ingredient) sodium hypochlorite (NaClO) for 15 s, rinsed twice in sterile distilled water (SDW) (30 s each), air-dried on sterile paper towels and placed onto water agar amended with streptomycin (0.1 mg mL^{-1}; WA-S) and potato dextrose agar amended with streptomycin (0.1 mg mL^{-1}; PDA-S) (Liu et al. 2025). For each tissue type, three replicate plates of each medium were prepared to maximise the chance of isolating *F. oxysporum*. Plates were incubated at 24°C under continuous light and checked for fungal growth every 24 h for a week. Representative colonies displaying typical *F. oxysporum*-like morphology (white to pink mycelium and purple pigmentation) (Adhikari et al. 2020) from each plant organ were subcultured onto PDA-S.

For isolation from the irrigation water samples, each sample was dispensed into four 50 mL Falcon tubes under aseptic conditions. Although *F. oxysporum* is traditionally regarded as a soil-borne pathogen, previous studies have demonstrated its capacity to survive in irrigation water and to infect host plants via water-mediated root contact (Joshi 2018; Ullah et al. 2021). To recover viable pathogenic isolates from water samples, a seedling baiting approach was employed. Eight 2-week-old healthy tomato seedlings grown on sterile water agar were used per water sample. Seedlings were derived from commercially imported seed certified under Australian biosecurity regulations and surface-sterilised prior to germination to minimise the risk of seed-borne contamination. The baiting protocol was adapted from Callaghan et al. (2022), which has been successfully applied for the recovery of plant pathogens from aquatic environments including irrigation water. Tubes were sealed

TABLE 1 | *Fusarium oxysporum* isolates from tomato (*Solanum lycopersicum*) fields in Australia, and the GenBank accession numbers for gene sequences used in phylogenetic analyses.

				GenBank accession number			
Isolate accession[a]	**Origin**	**Year**	**Source**[b]	***tub2***	***cmdA***	***rpb2***	***tef1-α***
BRIP 5188; UOM 25087	Stanthorpe, QLD	1971	n.d.	PV746104	PV746024	PV746064	PV745984
BRIP 13037; UOM 25088	Bowen, QLD	1979	n.d.	PV746105	PV746025	PV746065	PV745985
BRIP 16848; UOM 25089	Brisbane, QLD	1970	n.d.	PV746106	PV746026	PV746066	PV745986
BRIP 17552; UOM 25090	Stanthorpe, QLD	1980	n.d.	PV746107	PV746027	PV746067	PV745987
BRIP 76478; UOM 24033	Himba east, VIC	2022	C	PV746108	PV746028	PV746068	PV745988
BRIP 76479; UOM 24034	Himba east, VIC	2022	R	PV746109	PV746029	PV746069	PV745989
BRIP 76480; UOM 24035	Himba east, VIC	2022	S	PV746110	PV746030	PV746070	PV745990
BRIP 76481; UOM 24036	Thyra, NSW	2022	S	PV746111	PV746031	PV746071	PV745991
BRIP 76482; UOM 24037	Thyra, NSW	2022	R	PV746112	PV746032	PV746072	PV745992
BRIP 76483; UOM 24038	Rochester, VIC	2022	C	PV746113	PV746033	PV746073	PV745993
BRIP 76484; UOM 24039	Rochester, VIC	2022	C	PV746114	PV746034	PV746074	PV745994
BRIP 76485; UOM 24040	Rochester, VIC	2022	C	PV746115	PV746035	PV746075	PV745995
BRIP 76486; UOM 24041	Rochester, VIC	2022	C	PV746116	PV746036	PV746076	PV745996
BRIP 76487; UOM 24042	Rochester, VIC	2022	R	PV746117	PV746037	PV746077	PV745997
BRIP 76488; UOM 24043	Nanneella, VIC	2023	C	PV746118	PV746038	PV746078	PV745998
BRIP 76489; UOM 24044	Nanneella, VIC	2023	R	PV746119	PV746039	PV746079	PV745999
BRIP 76490; UOM 24045	Rochester, VIC	2023	C	PV746120	PV746040	PV746080	PV746000
BRIP 76491; UOM 24046	Rochester, VIC	2023	R	PV746121	PV746041	PV746081	PV746001
BRIP 76492; UOM 24047	Rochester, VIC	2023	S	PV746122	PV746042	PV746082	PV746002
BRIP 76493; UOM 24048	Thyra, NSW	2023	C	PV746123	PV746043	PV746083	PV746003
BRIP 76494; UOM 24049	Birganbigil, NSW	2023	S	PV746124	PV746044	PV746084	PV746004
BRIP 76495; UOM 24050	Thyra, NSW	2023	I	PV746125	PV746045	PV746085	PV746005
BRIP 76496; UOM 24051	Thyra, NSW	2023	I	PV746126	PV746046	PV746086	PV746006
BRIP 76497; UOM 24052	Thyra, NSW	2023	I	PV746127	PV746047	PV746087	PV746007
BRIP 76498; UOM 24053	Thyra, NSW	2023	I	PV746128	PV746048	PV746088	PV746008
BRIP 76499; UOM 24054	Thyra, NSW	2022	R	PV746129	PV746049	PV746089	PV746009
BRIP 76500; UOM 24055	Appin, VIC	2017	R	PV746130	PV746050	PV746090	PV746010
BRIP 76501; UOM 24056	Burramboot, VIC	2018	R	PV746131	PV746051	PV746091	PV746011
BRIP 76502; UOM 24057	Leaghur, VIC	2018	R	PV746132	PV746052	PV746092	PV746012
UOM 25002	Burramboot, VIC	2024	C	PV746133	PV746053	PV746093	PV746013
UOM 25003	Burramboot, VIC	2024	R	PV746134	PV746054	PV746094	PV746014
UOM 25004	Burramboot, VIC	2024	C	PV746135	PV746055	PV746095	PV746015
UOM 25005	Burramboot, VIC	2024	S	PV746136	PV746056	PV746096	PV746016
UOM 25006	Burramboot, VIC	2024	R	PV746137	PV746057	PV746097	PV746017
UOM 25007	Burramboot, VIC	2024	C	PV746138	PV746058	PV746098	PV746018
UOM 25008	Burramboot, VIC	2024	S	PV746139	PV746059	PV746099	PV746019

(Continues)

TABLE 1 | (Continued)

Isolate accession[a]	Origin	Year	Source[b]	GenBank accession number			
				tub2	*cmdA*	*rpb2*	*tef1-α*
UOM 25009	Burramboot, VIC	2024	C	PV746140	PV746060	PV746100	PV746020
UOM 25010	Burramboot, VIC	2024	S	PV746141	PV746061	PV746101	PV746021
UOM 25011	Burramboot, VIC	2024	R	PV746142	PV746062	PV746102	PV746022
UOM 25012	Burramboot, VIC	2024	C	PV746143	PV746063	PV746103	PV746023

Abbreviations: *cmdA*, calmodulin; *rpb2*, second largest subunit of nuclear RNA polymerase II; *tef1-α*, translation elongation factor 1-α; *tub2*, β-tubulin.
[a]BRIP, Queensland Plant Pathology Herbarium collection; UOM, The University of Melbourne Plant Pathology collection.
[b]n.d., not determined; C, collar; R, root; S, lower stem; I, irrigation water.

with surface-sterilised Parafilm, and a small opening was created to allow the seedling roots to be immersed directly in the water sample. After incubation for 2 weeks at room temperature, seedlings were harvested and fungal isolations from root tissues were conducted following the same procedures described above for plant material.

Single-spore isolation of each isolate was further conducted to establish pure cultures following the method described in Zhang et al. (2013). Four historical *F. oxysporum* isolates previously isolated from fresh tomato plants in Queensland (QLD) by Ramsey et al. (1992) were obtained from Queensland Plant Pathology Herbarium (BRIP, Brisbane) as reference Australian *F. oxysporum* isolates. Furthermore, one *F. oxysporum* isolate from 2017 and two from 2018 collected from processing tomato fields in a previous study (Callaghan 2020) were also included (Table 1).

2.2 | DNA Extraction, PCR and Sequencing

Genomic DNA from all isolates was extracted from mycelia of 7-day-old pure cultures growing on PDA. Mycelia were harvested using a sterile scalpel and transferred into 2 mL SafeLock tubes (Eppendorf), flash frozen in liquid nitrogen and freeze-dried (Ezzi Vision) for 48–72 h. Freeze-dried tissue was subsequently ground in a TissueLyser (Qiagen) into a fine powder using two steel balls (Sigma-Aldrich). Genomic DNA was isolated using a DNeasy Plant Mini Kit (Qiagen), following the manufacturer's instructions. The quality of the extracted DNA samples was assessed using a NanoDrop (Thermo Fisher Scientific) and DNA quantification was done using a Qubit fluorometer (Thermo Fisher Scientific). To evaluate the integrity of the DNA, agarose gel electrophoresis was conducted on 1% (w/v) agarose gel (in Tris acetate EDTA buffer) stained with SYBR Safe DNA Stain (Invitrogen) for visualisation.

The four genomic loci, *tub2*, *cmdA*, *rpb2* and *tef1-α*, were amplified for all isolates using primer pairs T1 (5′-AACATGCGTGAGATTGTAAGT-3′)/T2 (5′-TAGTGACCCT TGGCCCAGTTG-3′) (O'Donnell and Cigelnik 1997) for *tub2*, Cal228F (5′-GAGTTCAAGGAGGCCTTCTCCC-3′)/CAL2Rd (5′-TGRTCNGCCTCDCGGATCATCTC-3′)(Carbone and Kohn 1999) for *cmdA*, RPB2-5F2 (5′-GGGGWGAYCAGAAGAAGGC-3′)/RPB2-7cR (5′-CCCATRGCTTGTYYRCCCAT-3′) (Liu et al. 1999) for *rpb2* and EF1 (5′-ATGGGTAAGGA(A/G) GACAAGAC-3′)/EF2 (5′-GGA(G/A) GTACCAGT(G/C) ATCATGTT-3′) (O'Donnell et al. 1998) for *tef1-α*.

PCRs were adapted from the protocols described previously (Carbone and Kohn 1999; Lombard et al. 2019; O'Donnell et al. 1998). The final concentration in each 25 μL reaction included 0.4 μM of each forward and reverse primers, 6 ng template DNA (2 ng μL^{-1}), 1× PCR Master Mix (New England Biolabs), brought to volume by sterile Milli-Q water. The amplification reactions were performed in a thermal cycler (Eppendorf) with an initial denaturation for 9 min at 95°C; followed by 36 cycles of denaturation at 95°C for 30 s, annealing at 54°C for 45 s and extension at 68°C for 1 min (2 min for *rpb2*); and a final extension at 68°C for 5 min.

All PCR amplicons were visualised on 1% (w/v) agarose gels, stained with SYBR Safe DNA Gel Stain, to establish amplification of a single band of expected size. PCR products were submitted to Macrogen (Seoul, South Korea) for purification and Sanger sequencing in both forward and reverse directions using the same primers used for PCR. Quality control of raw data and generation of consensus sequences were conducted in Geneious Prime 2024.0.5 (http://www.geneious.com). All consensus sequences were deposited in NCBI GenBank database (Table 1).

2.3 | Phylogenetic Analyses

Three phylogenetic analyses were conducted based on different taxonomic frameworks. These included *tef1-α* single gene analysis containing reference sequences of *F. oxysporum* from O'Donnell et al. (1998) and Laurence et al. (2012); a combined four-gene phylogeny (*tub2*, *cmdA*, *rpb2* and *tef1-α*) with reference sequences of FOSC from Lombard et al. (2019); and the combined four-gene dataset with reference sequences of *F. oxysporum* from Achari et al. (2020).

The sequences of reference isolates were retrieved from GenBank for use in phylogenetic analyses. All sequence alignments were generated using the MAFFT plug-in in Geneious Prime 2025.1.3 (https://www.geneious.com). Maximum-likelihood (ML) analysis was conducted using RAxML plug-in in Geneious Prime, with 1000 pseudoreplicates and using GTRGAMMA nucleotide substitution model applied to separate partitions. Bayesian inference (BI) analysis was conducted using MrBayes v. 3.2.7a (Ronquist et al. 2012), and MrModeltest2 (Nylander et al. 2004) was used to determine the best-fit nucleotide substitutions models. Model test analysis resulted in an HKY+G model for the *tef1-α* single-gene

dataset containing reference sequences from O'Donnell et al. (1998) and Laurence et al. (2012). For the combined four-gene dataset with reference sequences from Lombard et al. (2019), the selected models were HKY+I+G for *tef1-α*, GTR+I+G for *rpb2*, K80+I for *cmdA* and K80+I+G for *tub2*. For the combined four-gene dataset with reference sequences from Achari et al. (2020), the selected models were K80 for *tef1-α*, SYM+G for *rpb2*, K80 for *cmdA* and HKY for *tub2*.

A neighbour-net algorithm was also used to construct a network implemented in SplitsTree using the four genomic loci (*tub2*, *cmdA*, *rpb2* and *tef1-α*), the uncorrected *p* distance and 1000 bootstraps (Huson and Bryant 2006). A phylogenetic network is more appropriate to depict incompatible and ambiguous signals in datasets and provide a more accurate representation of recombining datasets compared to tree-based models (Kajala et al. 2021). For this analysis, a subset of reference sequences was retrieved from Lombard et al. (2019) and Achari et al. (2020).

2.4 | Sequence Types

To depict genotypic diversity within phylogenetic clades better, DnaSP v. 5 was used to identify unique sequence types (haplotypes) for each of the four nuclear regions (single-locus haplotypes) and for combinations of the four loci (multilocus haplotypes) (Librado and Rozas 2009). Estimates of the number of segregating sites (S), haplotype diversity (H_d) and nucleotide diversity (π) were conducted for each locus separately and following concatenation of loci (Librado and Rozas 2009). Datasets were constructed to evaluate the taxonomic position of all haplotypes and their phylogenetic relationship to recognised *F. oxysporum* species based on the four genomic loci. All sequence alignments were generated using MAFFT plug-in in Geneious Prime as described before.

2.5 | Pathogenicity Bioassay

2.5.1 | Replicated Glasshouse Pathogenicity Bioassay

A subset of *F. oxysporum* isolates representing different clades in the phylogenetic analyses, UOM 24033, UOM 24034, UOM 24035, UOM 24036, UOM 24037, UOM 24055, UOM 24056 and UOM 24057, were selected from a total of 40 isolates for pathogenicity assays based on their four-gene haplotypes (Table S1).

Surface-sterilised seeds of a commonly grown processing tomato commercial cultivar (H3402 provided by the Australian Processing Tomato Research Council) were germinated in Seed Raising Mix (Plugger111, Australian Growing Solutions Pty Ltd.) for 2 weeks under 12 h of daylight at 25°C and 12 h of darkness at 20°C until the first pairs of true leaves emerged. For inoculation prior to planting, seedlings were dipped for 25 min into respective conidial suspensions (10^6 conidia mL^{-1}) prepared from eight selected *F. oxysporum* isolates for inoculated treatment. Mock-inoculated control seedlings were dipped in SDW for the same duration. Inoculation procedures followed those described in Feng et al. (2022).

The replicated pathogenicity bioassay was conducted in the University of Melbourne Glasshouse Complex with five internal replicates for each treatment. The experiment had nine treatments (eight *F. oxysporum* isolates and a mock-inoculated control), and a total number of 45 pots. All pots contained 1.5 kg of pasteurised potting mix (Plugger 111, Australian Growing Solutions Pty Ltd.), consisting of 90% composted substances, coarse bark, and 10% sand, which were arranged in a completely randomised design. Pots were placed under a 12 h photoperiod with a high-pressure sodium (HPS) light source and 25°C/20°C day/night temperatures for 8 weeks. Plants were watered every other day. A supplementary Osmocote fertiliser was applied according to the recommended rate to supply essential nutrients (Osmocote). All inoculated and control (mock-inoculated) plants were checked at the end of the experiment for re-isolation of *F. oxysporum* to verify pathogenicity in accordance with Koch's postulates (Liu et al. 2025). The experiment was repeated twice to confirm the repeatability of the results.

2.5.2 | Preliminary Pathogenicity Assessment of an Irrigation-Water-Derived Isolate

Fusarium oxysporum isolate UOM 24050 recovered from irrigation water was selected for a preliminary pathogenicity assay, as all four water-derived isolates clustered within the same phylogenetic lineage and shared an identical multilocus haplotype. The pathogenicity assay was conducted following the same glasshouse conditions described above for replicated pathogenicity experiments, using tomato cultivar H3402.

Inoculum was prepared following a modified protocol of Callaghan et al. (2022). For this, budgerigar millet seed mix (Trill) was soaked in tap water overnight and subsequently autoclaved twice at 121°C for 20 min in 14 half-filled 250 mL plastic containers on two consecutive days. Sterile seed contents in seven containers were inoculated with *F. oxysporum* isolate UOM 24050 by transferring several agar-plugs of 5- or 7-day-old cultures to the double-autoclaved seeds under aseptic conditions. Seven containers of seed were mock-inoculated with clean agar plugs as a negative control treatment. Containers were shaken thoroughly to ensure even distribution of the inoculum and incubated at room temperature for 4 weeks, until the millet seeds in inoculated treatment were fully colonised by *F. oxysporum*. After 4 weeks, the millet seed from each treatment was air-dried in a biosafety cabinet for 3 days, which were then thoroughly mixed by hand to ensure a uniform inoculum before the required quantity of seed was weighed to use as inoculum for glasshouse experiment. Due to limited replication, this assay was intended to qualitatively confirm pathogenicity rather than to enable quantitative comparison.

2.6 | Disease Assessment and Data Analysis

Disease assessment was conducted 8 weeks after inoculation of 10-week-old tomato plants. At harvest, above-ground plant height was measured, and root dry weights were determined after oven-drying at 70°C for 72 h (Liu et al. 2025). Physiological parameters, including stomatal conductance (g_s; mol H_2O $m^{-2}s^{-1}$), transpiration (E; mmol H_2O $m^{-2}s^{-1}$), and

photosynthesis (A; μmol CO_2 $m^{-2}s^{-1}$), were measured using a Li-6400 XT open gas exchange system (Li-Cor Inc.) (Feng et al. 2022). Measurements were taken from the youngest fully expanded leaves and repeated in different leaves of each plant ($n = 10$ per treatment, $n = 90$ in total). These measurements were taken at weeks 2 and 6 during the glasshouse pathogenicity bioassay, but not at week 0/day 0 (the day of transplanting) due to seedlings being fragile with very small leaf sizes.

Plant root dry weight, above-ground height and physiological response data were checked for normality and homogeneity of variance. Once these assumptions were met, data were analysed using one-way ANOVA, followed by Tukey's honestly significant difference (HSD) post hoc tests ($\alpha = 0.05$) using Minitab 2019.1.0 (Minitab) to assess significant differences between treatments.

3 | Results

3.1 | Sample Collection and Pathogen Isolation

A total of 33 *F. oxysporum* isolates were obtained from the 28 tomato plants and the six irrigation water samples from processing tomato fields in NSW and VIC, Australia (Table 1). These included 13 isolates from collar tissues, seven from lower stem and nine from root, as well as four isolates from irrigation water. Together with the three isolates from 2017 and 2018 (Callaghan 2020), we refer to these subsequently as the UOM isolates.

3.2 | Phylogenetic Analyses

The *tef1-α* alignment including reference isolates from O'Donnell et al. (1998) and Laurence et al. (2012) was 582 bp long and included 85 sequences. Both the ML and BI methods generated similar tree topologies; therefore, the ML tree is displayed, and BI-derived posterior probabilities were added to the ML tree (Figure 2). Most isolates clustered with reference FOSC isolates of Clade 2 and Clade 3, with low to high bootstrap support values (48%–95%) and moderate to high Bayesian posterior probability support (0.56–1.0). Reference isolates obtained from Queensland Plant Pathology Herbarium, BRIP 5188, BRIP 13037, BRIP 16848 and BRIP 17552, and three UOM isolates, UOM 25009, UOM 24036 and UOM 24034, did not cluster with any known clades. According to the combined phylogeny, 16 isolates clustered into Clade 2 with maximum Bayesian posterior probability support, while 17 isolates clustered in Clade 3 with maximum Bayesian posterior probability (Figure 2).

The four-gene dataset with reference sequences of FOSC from Lombard et al. (2019) included a concatenated alignment of *tub2*, *cmdA*, *rpb2* and *tef1-α* sequences with a total length of 2211 bp (*tub2* = 425 bp, *cmdA* = 385 bp, *rpb2* = 868 bp and *tef1-α* = 533 bp). Given the similarity in tree structures produced by both BI and ML methods, the posterior probabilities calculated from the BI analysis were integrated into the ML tree (Figure 3). Eight major clades were established, with the majority of UOM isolates clustering in Clades III, VI and VIII, and four UOM isolates clustering in Clade I, with no UOM isolates within Clades II, IV, V or VII. Clades III, VI and VIII exhibited the highest Bayesian posterior probability support of 0.93–1.0, and Clades I, III and VIII had Bayesian support values of 0.51–1.0. All four BRIP isolates retrieved from Queensland Plant Pathology Herbarium clustered within Clade VI, with reference isolates of *F. languescens*.

The four-gene dataset, including reference sequences from Achari et al. (2020), resulted in a concatenated alignment of 1959 bp (*tub2* = 413 bp, *cmdA* = 402 bp, *rpb2* = 930 bp and *tef1-α* = 214 bp). Given the similarity in tree topologies produced by both BI and ML methods, the posterior probabilities calculated from the BI analysis were integrated into the ML tree (Figure 4). Five UOM isolates clustered in Clade 1 described by Achari et al. (2020) with low ML bootstrap support (63%) but maximum Bayesian posterior probability. Sixteen UOM isolates clustered into Clade 2 with ML bootstrap support of 66% and a Bayesian posterior probability of 0.99. Nineteen UOM isolates clustered in Clade 3 with high ML bootstrap support (87%) and Bayesian posterior probability value (0.83).

The neighbour-net phylogenetic network constructed from the four genomic loci (*tub2*, *cmdA*, *rpb2* and *tef1-α*) including a subset of reference sequences from Achari et al. (2020) and Lombard et al. (2019) further resolved the FOSC isolates into three well-defined clades (Figure 5). Clade 1 (red) was composed of the tomato-associated reference isolate VPRI 41281 *Solanum lycopersicum*, and five UOM isolates, with moderate support value of 56%. Clade 2 (green) included *F. elaeidis*, *F. fabacearum* and *F. carminascens*, which contained 16 UOM isolates, supported by bootstrap values ranging from 56% to 74%. Clade 3 (blue) included *F. pharetum*, *F. veterinarium* and *F. curvatum*, along with numerous UOM and all BRIP reference isolates, with strong support for major internal nodes (87%, 95% and 97%). Lower support values were observed at deeper nodes, reflecting reticulation among clades.

3.3 | Multilocus Haplotypes and Estimates of Genetic Variation

Sequencing the *tub2*, *cmdA*, *rpb2* and *tef1-α* regions for 36 UOM *F. oxysporum* isolates collected from processing tomato fields in NSW and VIC, as well as the four reference BRIP isolates, detected 46 polymorphic sites and 27 haplotypes in the combined data of the four gene sequences and a total alignment length of 2200 bp (Table 2 and Table S1). For each gene sequence, the most frequent haplotype for *tub2* was *tub2*-Hap 1 that included 28 isolates with all BRIP isolates present, followed by *tub2*-Hap 2 that contained five isolates. For *cmdA*, the most frequent haplotype was *cmdA*-Hap 1 with 20 isolates in total, followed by *cmdA*-Hap 2, which included 17 isolates. For *rpb2*, the most frequent haplotype was *rpb2*-Hap 3 that contained 14 isolates, followed by *rpb2*-Hap 6, which included eight isolates. The most frequent *tef1-α* haplotype (*tef1-α*-Hap 5) included 14 isolates, followed by *tef1-α*-Hap 2 that contained eight isolates. The highest degree of sequence polymorphism was detected in the *tef1-α* region with a nucleotide diversity of 0.009 (Table 2). Detailed haplotypes of the four genomic loci of the 40 isolates are provided in Table S1.

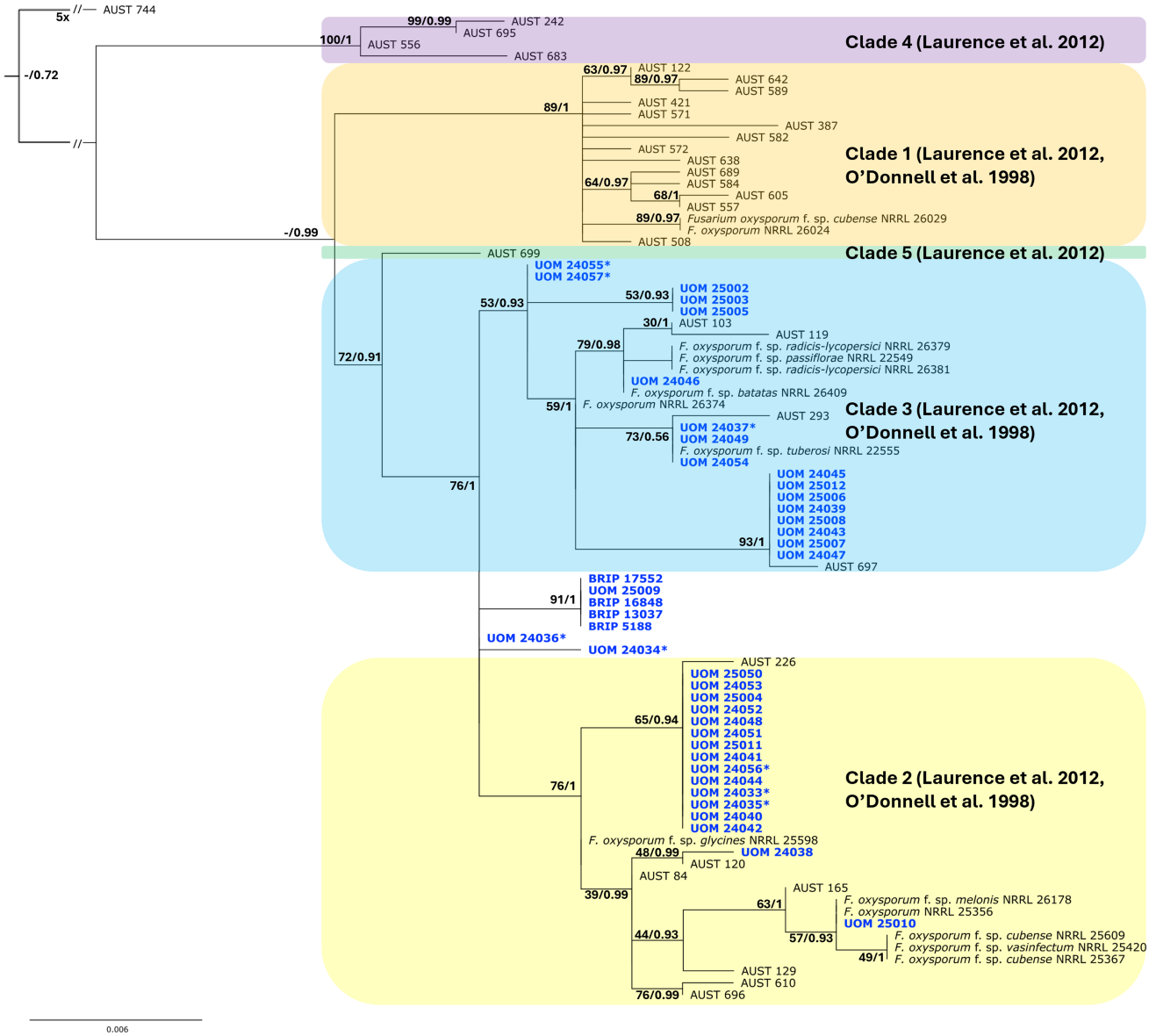

FIGURE 2 | A maximum-likelihood (ML) phylogeny of *Fusarium oxysporum* isolates inferred from the *tef1-α* alignment. The 40 isolates from tomato fields, sequenced in this study, are shown in bold blue. Reference taxa were chosen to represent the species level diversity in the *F. oxysporum* species complex (FOSC) classified by O'Donnell et al. (1998) (NRRL isolates) and clade level diversity in the FOSC classified by Laurence et al. (2012) (accession numbers starting with AUST). Clade information based on Laurence et al. (2012) and O'Donnell et al. (1998) is shown on the right. The ML bootstrap support (bs) values and Bayesian posterior probability (pp) values are indicated at nodes (bs/pp). The scale bar shows the number of nucleotide changes per site. The tree was rooted with AUST 774. Isolates labelled with an asterisk were used in the pathogenicity bioassay.

3.4 | Pathogenicity and Aggressiveness of *F. oxysporum* on Processing Tomato

Koch's postulates were satisfied. All inoculated processing tomato plants exhibited reduced growth compared with the control, whereas control plants remained healthy. The pathogen was consistently re-isolated from inoculated plants and confirmed as *F. oxysporum* based on culture morphology identical to the original isolates. Above-ground height of inoculated plants ranged from 35.60 ± 0.29 to 42.5 ± 0.21 cm, compared with 47.9 ± 0.39 cm in the control. Root development was similarly reduced, with dry root weights ranging from 1.23 ± 0.19 to 3.89 ± 0.10 g in inoculated plants and 7.01 ± 0.28 g in the control (Table 3). These reductions were significant ($p < 0.05$) regardless of the genetic background of the isolates. Furthermore, plant physiological responses were significantly reduced in all inoculated plants compared with the control (mock-inoculated treatment) at both measurement times (weeks 2 and 6; $p < 0.05$; Table 4). Photosynthesis ranged from 9.85 ± 0.16 to 13.39 ± 0.20 μmol CO_2 m^{-2} s^{-1} at week 2 and 3.79 ± 0.13 to 12.67 ± 0.13 μmol CO_2 m^{-2} s^{-1} at week 6 (control: 14.47 ± 0.29 and 14.94 ± 0.12, respectively). Transpiration ranged from 3.29 ± 0.10 to 4.78 ± 0.11 mmol H_2O m^{-2} s^{-1} at week 2 and 2.00 ± 0.09 to 4.53 ± 0.11 mmol H_2O m^{-2} s^{-1} at week 6 (control: 5.07 ± 0.14 and 6.15 ± 0.10), while stomatal conductance ranged from 0.43 ± 0.11 to 0.90 ± 0.07 mol H_2O m^{-2} s^{-1} at week 2 and 0.31 ± 0.01 to 0.67 ± 0.01 mol H_2O m^{-2} s^{-1} at week 6 (control: 1.25 ± 0.11 and 0.98 ± 0.04). Similar

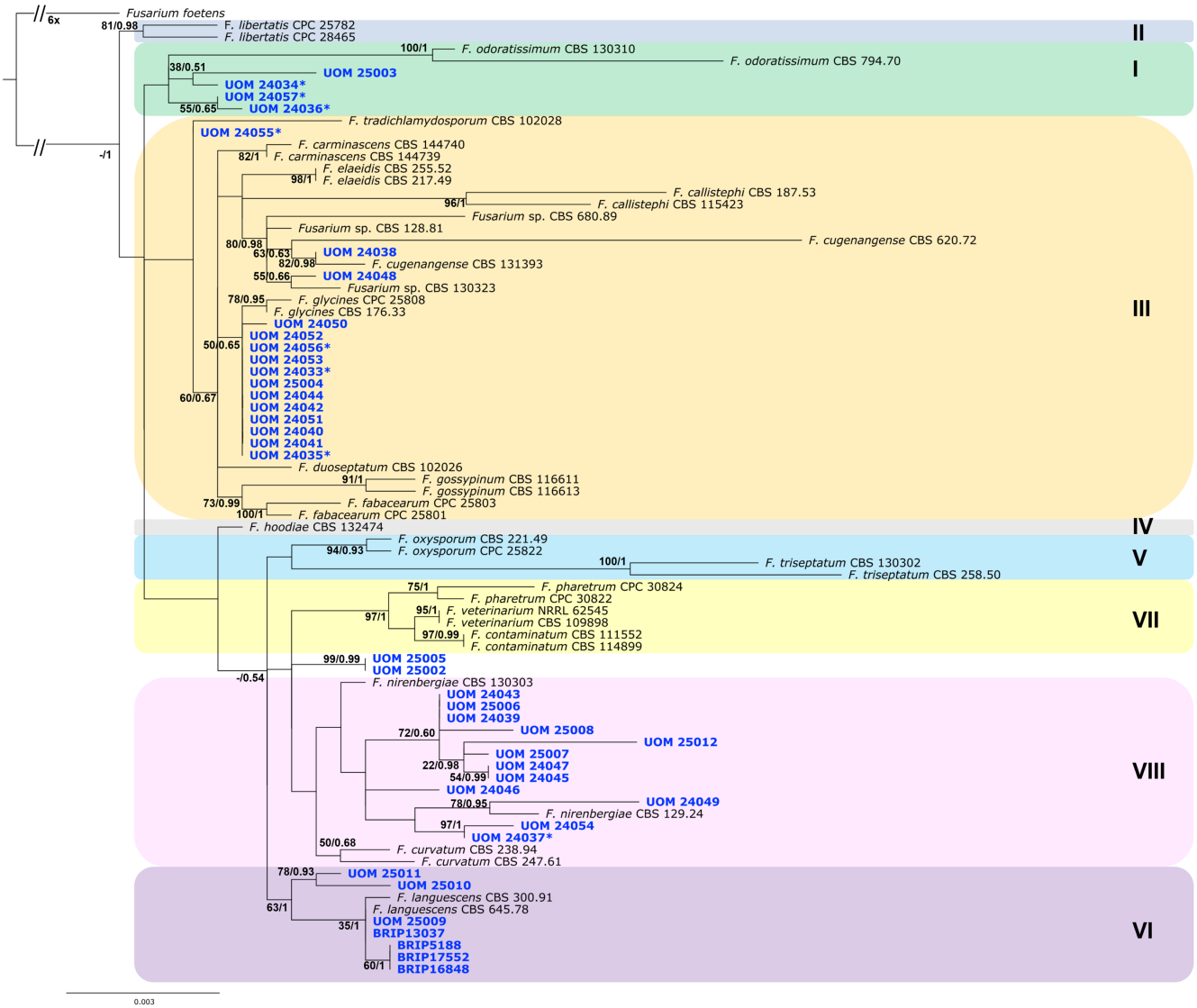

FIGURE 3 | A maximum-likelihood (ML) phylogeny of *Fusarium oxysporum* isolates inferred from concatenated alignment of *tub2*, *cmdA*, *rpb2* and *tef1-α* sequences. Reference taxa were chosen to represent the species level diversity in the *F. oxysporum* Species Complex (FOSC) classified by Lombard et al. (2019). The 40 isolates from tomato fields, sequenced in this study, are shown in bold blue. The ML bootstrap support (bs) values and Bayesian posterior probability (pp) values are indicated at the nodes (bs/pp). The scale bar shows the number of nucleotide changes per site. The tree was rooted with *Fusarium foetens*. Isolates labelled with an asterisk were used in the pathogenicity bioassay.

trends were observed at both time points, with all reductions being statistically significant. Among the eight *F. oxysporum* isolates tested in the pathogenicity bioassay, plants inoculated with UOM 24034 showed the highest root dry weight, above-ground height and physiological parameters among inoculated plants, indicating it was the least aggressive isolate. In contrast, plants inoculated with UOM 24055 showed the lowest values for these traits, making it the most aggressive isolate of those tested (Tables 3 and 4). Additionally, the representative *F. oxysporum* isolate UOM 24050 recovered from irrigation water was pathogenic on tomato. Infected seedlings developed symptoms consistent with *F. oxysporum* infection, including leaf chlorosis, defoliation and early wilting compared with mock-inoculated controls. Because this assay was conducted with limited replication, data were not included for quantitative comparison due to differing experimental conditions.

Despite the variability in aggressiveness among isolates, only two inoculated plants exhibited minor internal lesions in the lower stems under glasshouse conditions. No other visible lesions or discolourations were observed. Nevertheless, all inoculated plants showed significant reductions in above-ground growth, root production and physiological parameters, demonstrating that the tested isolates were pathogenic under glasshouse conditions.

4 | Discussion

Phylogenetic analyses of four genomic loci in FOSC isolates collected from processing tomato fields in Australia revealed substantial genetic diversity and genetic exchange among clades, highlighting the complexity of their taxonomic placement. Isolates were placed across different clades within the FOSC,

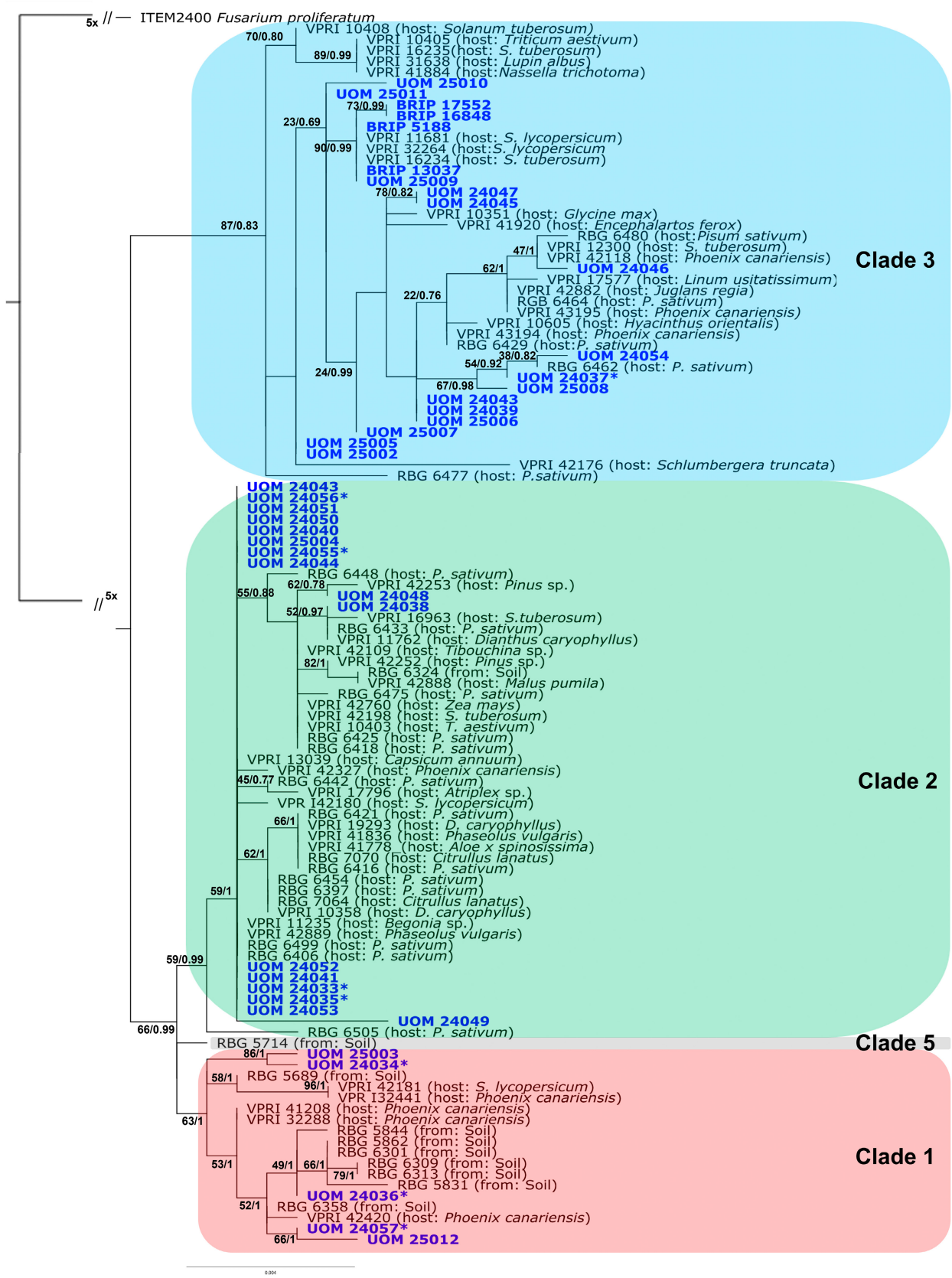

FIGURE 4 | A maximum-likelihood (ML) phylogeny of *Fusarium oxysporum* isolates inferred from the concatenated alignment of *tub2*, *cmdA*, *rpb2* and *tef1-α* sequences. Reference taxa were chosen to represent the species level diversity in the FOSC classified by Achari et al. (2020). The 40 isolates from tomato fields, sequenced in this study, are shown in blue bold. The ML bootstrap support (bs) values and Bayesian posterior probability (pp) values are indicated at nodes (bs/pp). The scale bar shows the number of nucleotide changes per site. The tree was rooted with ITEM 2400 *F. proliferatum*. Isolates labelled with an asterisk were used in the pathogenicity bioassay.

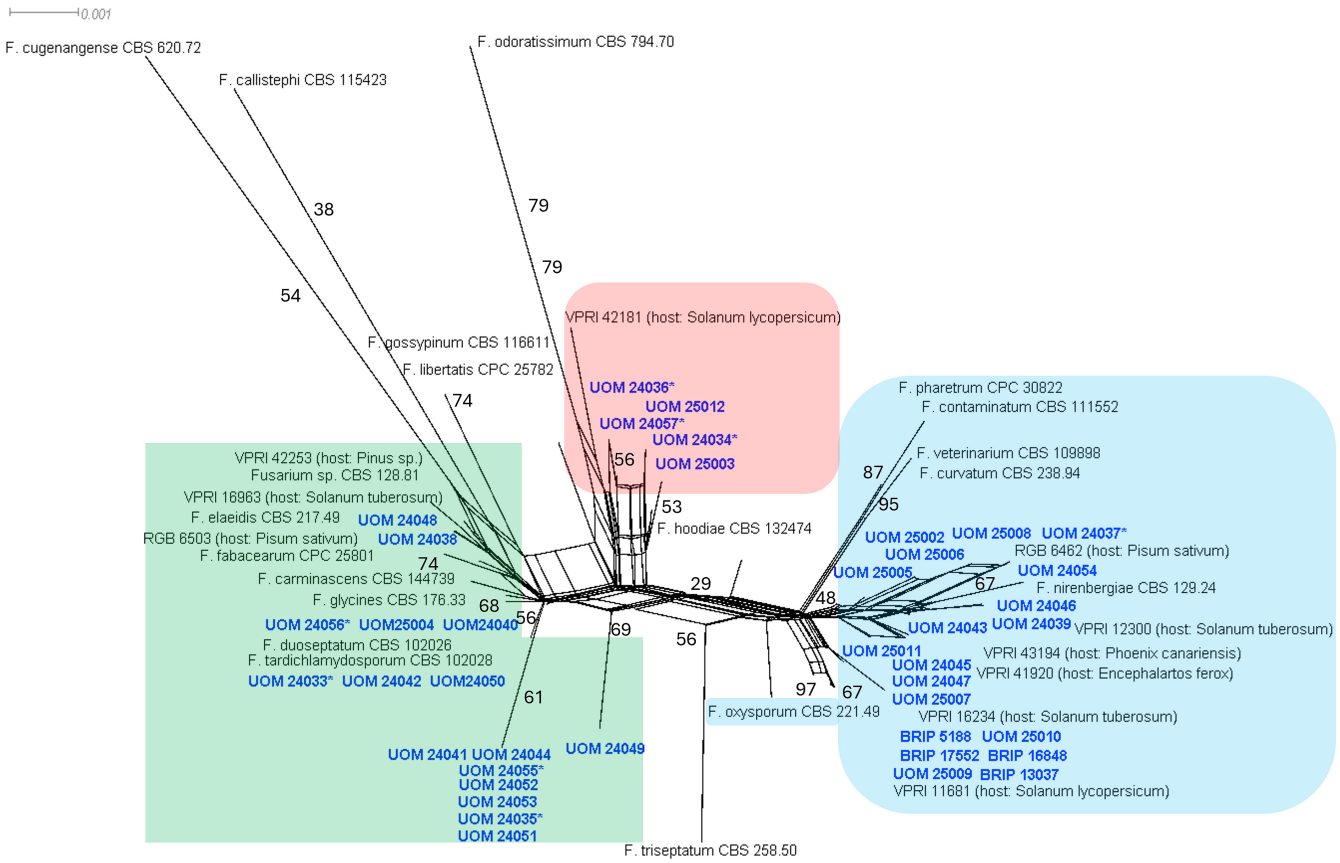

FIGURE 5 | Phylogenetic relationships among *Fusarium oxysporum* isolates based on concatenation of four genomic loci (*tub2*, *cmdA*, *rpb2* and *tef1-α*). Shown in blue are isolates collected from processing tomato fields in New South Wales and Victoria, and the four reference isolates (BRIP) from fresh tomato in Queensland. Shown in black are reference isolates from Lombard et al. (2019) and Achari et al. (2020). The scale bar represents the expected changes per site. Isolates with an asterisk were used in the pathogenicity bioassay. Red, green and blue boxes represent Clades 1, 2 and 3 based on the phylogenetic analyses proposed by Achari et al. (2020).

TABLE 2 | Summary statistics of DNA polymorphism in four nuclear loci (*tub2*, *cmdA*, *rpb2* and *tef1-α*) sequenced in this study of 40 *Fusarium oxysporum* isolates from tomato in Australia.

Locus	*tub2*	*cmdA*	*rpb2*	*tef1-α*	Combined
No. of sites	415	362	893	530	2200
S	3	3	20	20	46
H	3	4	11	10	24
H_d	0.304	0.581	0.832	0.818	0.908
π	0.0009	0.0018	0.0056	0.0091	0.0049
D	−1.0624 n.s.	−0.1432 n.s.	0.2349 n.s.	−0.1234 n.s.	−0.0769 n.s.

Note: S, number of polymorphic sites (number of parsimony informative sites); *H*, number of haplotypes; H_d, haplotype diversity; π, nucleotide diversity defined as the average number of nucleotide differences per site between any two randomly chosen DNA sequences; *D*, Tajima's *D*; n.s., not significant, $p > 0.05$.

suggesting the potential involvement of multiple phylogenetic species in yield decline in processing tomato.

Species assignment within the FOSC is complicated by the complex evolutionary history of isolates as revealed through extensive reticulation, most probably driven by frequent horizontal gene transfer and recombination, and also the use of differing taxonomic frameworks in FOSC taxonomy. Based on the four-gene phylogeny proposed by Lombard et al. (2019), the isolates were assigned to at least eight species within the FOSC. In contrast, the systems proposed by O'Donnell et al. (1998) and Laurence et al. (2012) placed these isolates within two of the three (O'Donnell et al. 1998) and five clades (Laurence et al. 2012), respectively, while the application of the methodology proposed by Achari et al. (2020) assigned them to four clades. Despite variations among different taxonomic frameworks, multilocus phylogenetic and coalescent-based analyses, including nuclear, mitochondrial and genome-wide datasets, have consistently aligned with earlier studies that support the division of the FOSC into three major clades (Aoki

TABLE 3 | Mean (± SE) values of root dry weight and above-ground height of processing tomato plants 8 weeks after inoculation with *Fusarium oxysporum* isolates.

Treatment	Isolate haplotype[a]	Isolate source	Root dry weight (g) ± SE	Above-ground height (cm) ± SE
Control	—	—	7.01 ± 0.28 A	47.90 ± 0.39 A
UOM 24033	16	Collar	1.57 ± 0.09 C	37.80 ± 0.36 CDE
UOM 24034	24	Root	3.88 ± 0.10 B	42.50 ± 0.21 B
UOM 24035	4	Lower stem	1.92 ± 0.05 C	36.80 ± 0.35 DE
UOM 24036	5	Lower stem	1.86 ± 0.05 C	39.80 ± 0.27 BCD
UOM 24037	18	Root	2.14 ± 0.12 C	39.40 ± 0.17 BCD
UOM 24055	2	Root	1.23 ± 0.19 C	35.60 ± 0.29 E
UOM 24056	16	Root	1.71 ± 0.18 C	37.20 ± 0.26 DE
UOM 24057	1	Root	1.63 ± 0.20 C	40.60 ± 0.28 BC

Note: Different uppercase letters show significant differences between treatments (rows) based on ANOVA and Tukey's honestly significant difference (HSD) post hoc tests ($\alpha = 0.05$; $p < 0.05$).
[a]Haplotypes refer to the unique sequence types for the four-locus haplotype for each isolate (Tables 2 and Table S1).

TABLE 4 | Mean (± SE) values of tomato plant physiological parameters in response to inoculation with *Fusarium oxysporum* isolates at 2 and 6 weeks post-inoculation (wpi).

	Photosynthesis (μmol CO_2 $m^{-2}s^{-1}$) ± SE		Stomatal conductance (mol H_2O $m^{-2}s^{-1}$) ± SE		Transpiration (mmol H_2O $m^{-2}s^{-1}$) ± SE	
Treatment	2 wpi	6 wpi	2 wpi	6 wpi	2 wpi	6 wpi
Control	14.47 ± 0.29 A	14.94 ± 0.12 A	1.25 ± 0.11 A	0.98 ± 0.04 A	5.07 ± 0.14 A	6.15 ± 0.10 A
UOM 24033	9.89 ± 0.16 F	5.48 ± 0.15 F	0.50 ± 0.06 CD	0.41 ± 0.01 E	3.65 ± 0.06 D	3.21 ± 0.08 E
UOM 24034	13.39 ± 0.20 B	12.67 ± 0.13 B	0.90 ± 0.07 B	0.67 ± 0.01 B	4.55 ± 0.16 BC	4.53 ± 0.11 B
UOM 24035	10.71 ± 0.18 DEF	10.18 ± 0.19 D	0.59 ± 0.01 CD	0.57 ± 0.01 C	4.42 ± 0.13 BC	3.90 ± 0.04 CD
UOM 24036	11.04 ± 0.05 D	9.93 ± 0.14 D	0.57 ± 0.01 CD	0.56 ± 0.01 CD	4.13 ± 0.05 C	3.89 ± 0.04 CD
UOM 24037	12.24 ± 0.20 C	11.46 ± 0.14 C	0.70 ± 0.02 BC	0.65 ± 0.01 B	4.78 ± 0.11 AB	4.22 ± 0.06 BC
UOM 24055	9.85 ± 0.16 F	3.79 ± 0.13 G	0.48 ± 0.01 CD	0.31 ± 0.01 F	3.29 ± 0.10 D	2.00 ± 0.09 F
UOM 24056	10.81 ± 0.18 DE	10.00 ± 0.28 D	0.60 ± 0.01 CD	0.57 ± 0.01 C	4.29 ± 0.03 C	3.98 ± 0.06 C
UOM 24057	9.99 ± 0.27 EF	9.10 ± 0.05 E	0.43 ± 0.11 D	0.50 ± 0.01 D	4.26 ± 0.07 C	3.60 ± 0.08 D

Note: Different uppercase letters show significant differences between treatments (rows) based on ANOVA and Tukey's honestly significant difference (HSD) post hoc tests ($\alpha = 0.05$; $p < 0.05$).

et al. 2014; Brankovics et al. 2017; Laurence et al. 2012), two of which encompassed the tomato-associated isolates.

In addition to the genetic diversity observed through tree-based analyses, the phylogenetic network analysis further highlighted the substantial genetic complexity within the FOSC with three well-defined clades. These results indicate that the tested isolates represent diverse phylogenetic lineages within the FOSC and align more closely with the three-clade classification than with the eight-clade taxonomy proposed by Lombard et al. (2019). The extensive reticulation among isolates indicates exchange of genetic material among clades potentially through recombination and horizontal gene transfer. This is consistent with previous studies, which have reported similar reticulated network patterns reflecting recombination and gene flow within the FOSC (Fayyaz et al. 2023; Hoogendoorn et al. 2018). The detection of genetic exchange across diverse clades underscores the evolutionary flexibility of *F. oxysporum* and poses further challenges for species delimitation, diagnostics and disease management strategies. While our results show the presence of at least two phylogenetic species within the tomato-associated FOSC isolates, we refrain from describing separate species or *formae speciales* due to the absence of evidence for ecological or host separation among the isolates and the lack of consistency across different approaches.

Multilocus haplotype analysis revealed that all four isolates obtained from irrigation water samples, UOM 24050, UOM 24051, UOM 24052 and UOM 24053, were assigned to Hap-16, the most frequently observed haplotype isolated from tomato plants based on the combined four-gene sequence dataset (Table S1). The occurrence of a dominant haplotype in irrigation water indicates that recycled irrigation water from a single processing

tomato field may serve as a source of *F. oxysporum* inoculum contributing to disease epidemics. Although *F. oxysporum* is traditionally regarded as a soil-borne pathogen, members of the FOSC are capable of persisting in aquatic environments (Graça et al. 2016), potentially through the formation of stress-tolerant propagules such as chlamydospores, association with organic debris or survival on plant residues present in irrigation systems (Palmero et al. 2011). This suggests that contaminated irrigation water may contribute to the dissemination of clonal lineages within and across fields. Such a route of spread aligns with previous studies that have identified irrigation water as a critical factor in the epidemiology of *F. oxysporum* (Ullah et al. 2021), further underscoring the potential role of water-mediated dispersal of the dominant haplotype around processing tomato-growing regions.

The genetic diversity across the four gene regions analysed varied considerably, with *rpb2* and *tef1-α* showing greater diversity than *cmdA* and *tub2*. Specifically, *rpb2* exhibited the highest number of polymorphic sites (*S*), highest haplotype diversity (H_d) and second highest nucleotide diversity (π). *tef1-α* followed with the second highest H_d and π values, indicating a similarly high level of genetic variability. In contrast, *cmdA* and *tub2* displayed lower *S*, H_d and π values, pointing to lower resolution power of these loci for within-species diversity analyses. Previous studies have also found that *tef1-α* exhibited high sequence type diversity whereas *rpb2* provided high-resolution phylogenetic information, indicating significant genetic diversity (Nephalela-Mavhunga et al. 2021).

The replicated pathogenicity bioassay conducted under controlled glasshouse conditions confirmed that all eight isolates were pathogenic to the commercial processing tomato cultivar tested in Australia. Infected plants exhibited significantly reduced dry matter accumulation and impaired physiological responses. Reductions in photosynthesis rate, stomatal conductance and transpiration were observed in inoculated plants and are consistent with the growth reduction recorded in this study. These physiological changes are commonly associated with vascular wilt diseases, where xylem colonisation and impairment of water transport lead to reduced gas exchange (Deans et al. 2020), stomatal closure (Muir 2020) and diminished carbon assimilation (Verma et al. 2009). In the present study, declines in physiological performance broadly aligned with reductions in above-ground biomass and root development, supporting their use as indicators of disease impact rather than as standalone diagnostic traits.

Although pathogenicity testing of *F. oxysporum* isolates derived from irrigation water was limited in scope and replication, qualitative assessment of a representative Hap-16 isolate UOM 24050 confirmed its ability to cause disease on tomato. This finding supports the epidemiological relevance of irrigation systems as potential sources of viable inoculum associated with the dominant haplotype identified in processing tomato fields. Because this assessment was conducted under different experimental conditions and without accompanying physiological measurements, the results were not intended for quantitative comparison with replicated pathogenicity assays, but rather to demonstrate pathogenic potential of water-associated isolates.

Notably, the commercial cultivar tested here (cv. H3402), although reported to exhibit resistance to Fusarium wilt in the United States (Stewart 2023), did not show resistance to the Australian *F. oxysporum* isolates. Therefore, further screening and evaluation of imported processing tomato cultivars using Australian isolates are essential to identify and develop effective resistance against the diverse Australian *F. oxysporum* populations.

In addition, various degrees of aggressiveness were observed among the eight tested isolates, irrespective of their phylogenetic placement or genetic variation observed among the isolates across the three phylogenetic frameworks. This highlights that phylogenetic classification, which reflects genetic relatedness based on housekeeping loci, does not necessarily predict pathogenicity or aggressiveness. Pathogenicity depends on phenotypic assays, rather than sequence similarity alone. Consequently, assessing disease potential cannot rely solely on genomic sequences, and experimental evaluation of host–pathogen interactions remains essential. These findings are consistent with previous studies showing that genetic divergence among FOSC isolates did not always correspond to phenotypic or pathogenic differentiation sufficient to justify species-level distinctions (Manawasinghe et al. 2021).

Last but not least, classical race classifications of *F. oxysporum* f. sp. *lycopersici* (FOL) have been instrumental for resistance breeding; however, these frameworks are largely based on a limited number of well-characterised Northern Hemisphere lineages (Srinivas et al. 2019; Swett et al. 2023). Increasing evidence suggests that tomato-pathogenic *F. oxysporum* populations can be phylogenetically diverse and may fall outside canonical FOL clades while retaining high virulence. In such cases, race-associated markers and effector profiles may not reliably reflect evolutionary relationships or pathogenic potential. These observations reinforce the need for phylogeny-based approaches to understand pathogen diversity, particularly in under-studied regions such as Australia.

In conclusion, FOSC was demonstrated to be a dominant pathogen affecting processing tomato crops in Victoria and New South Wales, Australia. The inconsistent phylogenetic groupings derived from three analytical frameworks using identical genomic loci support the polyphyletic nature of the pathogen. A replicated glasshouse pathogenicity bioassay confirmed the field-observed growth reductions, although characteristic disease symptoms such as wilting, root rot and collar lesions were not consistently reproduced. Notably, all FOSC isolates tested caused statistically significant growth suppression on the most commonly used commercial cultivar H3402, indicating a lack of complete resistance regardless of isolate phylogeny. The successful isolation of *F. oxysporum* from irrigation water also highlights its potential role as a possible inoculum source in field epidemiology. These findings underscore the need for further investigation into the evolutionary origins and population structure of FOSC obtained in Australian processing tomato fields, along with its epidemiological dynamics, to improve host

resistance selection and inform more effective, regionally tailored disease management strategies.

Author Contributions

Sophia E. Callaghan: writing – review and editing, resources. **Yu Pei Tan:** writing – review and editing, resources. **Jiajing Cao:** writing – review and editing, resources. **Paul W. J. Taylor:** funding acquisition, writing – review and editing, project administration, supervision, resources. **Niloofar Vaghefi:** validation, visualization, writing – review and editing, data curation, supervision, resources. **Hanyue Feng:** conceptualization, investigation, writing – original draft, methodology, validation, visualization, writing – review and editing, software, formal analysis, data curation. **Sigfredo Fuentes:** writing – review and editing, supervision. **Alexis Pang:** writing – review and editing, supervision.

Acknowledgements

We appreciate the tremendous help and support from Matthew Stewart and Ann Morrison from the Australian Processing Tomato Research Council. Open access publishing facilitated by The University of Melbourne, as part of the Wiley - The University of Melbourne agreement via the Council of Australasian University Librarians.

Funding

This project is funded by the Australian Processing Tomato Research Council (APTRC). The first author gratefully appreciates the support of a Melbourne Research Scholarship provided by the University of Melbourne.

Conflicts of Interest

The authors declare no conflicts of interest.

Data Availability Statement

The data that support the findings of this study are deposited to public repositories and also available from the corresponding author upon reasonable request.

References

Achari, S. R., J. Kaur, Q. Dinh, et al. 2020. "Phylogenetic Relationship Between Australian *Fusarium oxysporum* Isolates and Resolving the Species Complex Using the Multispecies Coalescent Model." *BMC Genomics* 21: 248.

Adhikari, T. B., A. Gao, T. Ingram, and F. J. Louws. 2020. "Pathogenomics Characterization of an Emerging Fungal Pathogen, *Fusarium oxysporum* f. sp. *lycopersici* in Greenhouse Tomato Production Systems." *Frontiers in Microbiology* 11: 1995.

Afordoanyi, D. M., R. G. C. Diabankana, Y. A. Akosah, and S. Z. Validov. 2022. "Are *formae speciales* Pathogens Really Host Specific? A Broadened Host Specificity in *Fusarium oxysporum* f. sp. *radicis-cucumerinum*." *Brazilian Journal of Microbiology* 53: 1745–1759.

Aoki, T., K. O'Donnell, and D. M. Geiser. 2014. "Systematics of Key Phytopathogenic *Fusarium* Species: Current Status and Future Challenges." *Journal of General Plant Pathology* 80: 189–201.

Baayen, R. P., K. O'Donnell, P. J. Bonants, et al. 2000. "Gene Genealogies and AFLP Analyses in the *Fusarium oxysporum* Complex Identify Monophyletic and Nonmonophyletic *formae speciales* Causing Wilt and Rot Disease." *Phytopathology* 90: 891–900.

Brankovics, B., P. van Dam, M. Rep, et al. 2017. "Mitochondrial Genomes Reveal Recombination in the Presumed Asexual *Fusarium oxysporum* Species Complex." *BMC Genomics* 18: 735.

Callaghan, S. E. 2020. *Root and Collar Rot Pathogens Associated With Yield Decline of Processing Tomatoes in Victoria, Australia*. University of Melbourne. [Thesis].

Callaghan, S. E., L. W. Burgess, P. Ades, et al. 2018. "Progress in Understanding Soil-Borne Pathogens Associated With Poor Growth of Tomato Plants in the Australian Processing Tomato Industry." *Annual Processing Tomato Growers Magazine* 39: 10–13.

Callaghan, S. E., L. W. Burgess, P. Ades, L. A. Tesoriero, and P. W. J. Taylor. 2022. "Diversity and Pathogenicity of *Pythium* Species Associated With Reduced Yields of Processing Tomatoes (*Solanum lycopersicum*) in Victoria, Australia." *Plant Disease* 106: 1645–1652.

Cammarano, D., S. Jamshidi, G. Hoogenboom, A. C. Ruane, D. Niyogi, and D. Ronga. 2022. "Processing Tomato Production Is Expected to Decrease by 2050 due to the Projected Increase in Temperature." *Nature Food* 3: 437–444.

Carbone, I., and L. M. Kohn. 1999. "A Method for Designing Primer Sets for Speciation Studies in Filamentous Ascomycetes." *Mycologia* 91: 553–556.

Caruso, A. G., S. Bertacca, G. Parrella, R. Rizzo, S. Davino, and S. Panno. 2022. "Tomato Brown Rugose Fruit Virus: A Pathogen That Is Changing the Tomato Production Worldwide." *Annals of Applied Biology* 181: 258–274.

De Silva, D. D., P. K. Ades, and P. W. J. Taylor. 2021. "Pathogenicity of *Colletotrichum* Species Causing Anthracnose of Capsicum in Asia." *Plant Pathology* 70: 875–884.

Deans, R. M., T. J. Brodribb, F. A. Busch, and G. D. Farquhar. 2020. "Optimization Can Provide the Fundamental Link Between Leaf Photosynthesis, Gas Exchange and Water Relations." *Nature Plants* 6: 1116–1125.

Fayyaz, A., G. Robinson, P. L. Chang, et al. 2023. "Hiding in Plain Sight: Genome-Wide Recombination and a Dynamic Accessory Genome Drive Diversity in *Fusarium oxysporum* f. sp. *ciceris*." *Proceedings of the National Academy of Sciences of the United States of America* 120: e2220570120.

Feng, H., C. Gonzalez Viejo, N. Vaghefi, P. W. J. Taylor, E. Tongson, and S. Fuentes. 2022. "Early Detection of *Fusarium oxysporum* Infection in Processing Tomatoes (*Solanum lycopersicum*) and Pathogen–Soil Interactions Using a Low-Cost Portable Electronic Nose and Machine Learning Modeling." *Sensors* 22: 8645.

Graça, M. G., I. M. van der Heijden, L. Perdigão, C. Taira, S. F. Costa, and A. S. Levin. 2016. "Evaluation of Two Methods for Direct Detection of *Fusarium* spp. in Water." *Journal of Microbiological Methods* 123: 39–43.

Han, S., P. Zhao, M. Wang, et al. 2025. "What Is *Fusarium* Forma Specialis?" *Mycology* 16: 1522–1557.

Hoogendoorn, K., L. Barra, C. Waalwijk, J. S. Dickschat, T. A. J. van der Lee, and M. H. Medema. 2018. "Evolution and Diversity of Biosynthetic Gene Clusters in *Fusarium*." *Frontiers in Microbiology* 9: 1158.

Huson, D. H., and D. Bryant. 2006. "Application of Phylogenetic Networks in Evolutionary Studies." *Molecular Biology and Evolution* 23: 254–267.

Jangir, P., N. Mehra, K. Sharma, N. Singh, M. Rani, and R. Kapoor. 2021. "Secreted in Xylem Genes: Drivers of Host Adaptation in *Fusarium oxysporum*." *Frontiers in Plant Science* 12: 628611.

Joshi, R. 2018. "A Review of *Fusarium oxysporum* on Its Plant Interaction and Industrial Use." *Journal of Medicinal Plants Studies* 6: 112–115.

Kajala, K., M. Gouran, L. Shaar-Moshe, et al. 2021. "Innovation, Conservation, and Repurposing of Gene Function in Root Cell Type Development." *Cell* 184: 3333–3348.

Laurence, M. H., L. W. Burgess, B. A. Summerell, and E. C. Liew. 2012. "High Levels of Diversity in *Fusarium oxysporum* From Non-Cultivated Ecosystems in Australia." *Fungal Biology* 116: 289–297.

Librado, P., and J. Rozas. 2009. "DnaSP v5: A Software for Comprehensive Analysis of DNA Polymorphism Data." *Bioinformatics* 25: 1451–1452.

Lievens, B., M. Rep, and B. P. Thomma. 2008. "Recent Developments in the Molecular Discrimination of *formae speciales* of *Fusarium oxysporum*." *Pest Management Science* 64: 781–788.

Liu, Y., N. Vaghefi, A. Idnurm, P. K. Ades, and P. W. J. Taylor. 2025. "Aggressiveness and Phylogenetic Relationship of *Fusarium oxysporum* Associated With Crown and Root Rot in Pyrethrum Plants." *Plant Disease* 109: 1422–1433.

Liu, Y. J., S. Whelen, and B. D. Hall. 1999. "Phylogenetic Relationships Among Ascomycetes: Evidence From an RNA Polymerase II Subunit." *Molecular Biology and Evolution* 16: 1799–1808.

Lombard, L., M. Sandoval-Denis, S. C. Lamprecht, and P. W. Crous. 2019. "Epitypification of *Fusarium oxysporum* – Clearing the Taxonomic Chaos." *Persoonia* 43: 1–47.

Ma, M., P. W. J. Taylor, D. Chen, N. Vaghefi, and J.-Z. He. 2023. "Major Soilborne Pathogens of Field Processing Tomatoes and Management Strategies." *Microorganisms* 11: 263.

Manawasinghe, I. S., A. J. L. Phillips, J. Xu, et al. 2021. "Defining a Species in Fungal Plant Pathology: Beyond the Species Level." *Fungal Diversity* 109: 267–282.

McGovern, R. J. 2015. "Management of Tomato Diseases Caused by *Fusarium oxysporum*." *Crop Protection* 73: 78–92.

McKenzie, T. J., L. Singh-Peterson, and S. J. R. Underhill. 2017. "Quantifying Postharvest Loss and the Implication of Market-Based Decisions: A Case Study of Two Commercial Domestic Tomato Supply Chains in Queensland, Australia." *Horticulturae* 3: 44.

Muir, C. D. 2020. "A Stomatal Model of Anatomical Tradeoffs Between Gas Exchange and Pathogen Colonization." *Frontiers in Plant Science* 11: 518991.

Nephalela-Mavhunga, M., G. T. Kwinda, B. A. Summerell, E. Venter, and A. Jacobs. 2021. "Genetic Diversity of the *Fusarium oxysporum* Complex Isolated From the Grassland Biome of South Africa." *Phytopathology* 111: 1459–1469.

Nylander, J. A., F. Ronquist, J. P. Huelsenbeck, and J. L. Nieves-Aldrey. 2004. "Bayesian Phylogenetic Analysis of Combined Data." *Systematic Biology* 53: 47–67.

O'Donnell, K., and E. Cigelnik. 1997. "Two Divergent Intragenomic rDNA ITS2 Types Within a Monophyletic Lineage of the Fungus *Fusarium* Are Nonorthologous." *Molecular Phylogenetics and Evolution* 7: 103–116.

O'Donnell, K., H. C. Kistler, E. Cigelnik, and R. C. Ploetz. 1998. "Multiple Evolutionary Origins of the Fungus Causing Panama Disease of Banana: Concordant Evidence From Nuclear and Mitochondrial Gene Genealogies." *Proceedings of the National Academy of Sciences of the United States of America* 95: 2044–2049.

Palmero, D., J. M. Rodríguez, M. de Cara, F. Camacho, C. Iglesias, and J. C. Tello. 2011. "Fungal Microbiota From Rain Water and Pathogenicity of *Fusarium* Species Isolated From Atmospheric Dust and Rainfall Dust." *Journal of Industrial Microbiology and Biotechnology* 38: 13–20.

Ramsey, M., R. O'Brien, and K. Pegg. 1992. "*Fusarium oxysporum* Associated With Wilt and Root Rot of Tomato in Queensland; Races and Vegetative Compatibility Groups." *Australian Journal of Experimental Agriculture* 32: 651–655.

Ronquist, F., M. Teslenko, P. van der Mark, et al. 2012. "MrBayes 3.2: Efficient Bayesian Phylogenetic Inference and Model Choice Across a Large Model Space." *Systematic Biology* 61: 539–542.

Srinivas, C., D. Nirmala Devi, K. Narasimha Murthy, et al. 2019. "*Fusarium oxysporum* f. sp. *lycopersici* Causal Agent of Vascular Wilt Disease of Tomato: Biology to Diversity – A Review." *Saudi Journal of Biological Sciences* 26: 1315–1324.

Stewart, M. 2023. "Annual Industry Survey 2023." *Australian Processing Tomato Grower* 44: 28–36.

Swett, C. L., J. Del Castillo Múnera, E. Hellman, et al. 2023. "Monitoring for a New *I3* Resistance Gene-Breaking Race of *F. oxysporum* f. sp. *lycopersici* (Fusarium Wilt) in California Processing Tomatoes Following Recent Widespread Adoption of Resistant (F3) Cultivars: Challenges With Race 3 and 4 Differentiation Methods." *Frontiers in Plant Science* 14: 1088044.

Ullah, S., D. Mostert, K. Serfontein, and A. Viljoen. 2021. "The Survival and Treatment of *Fusarium oxysporum* f. sp. *cubense* in Water." *Journal of Fungi* 7: 796.

Verma, A., B. Kaur, C. Malik, Y. Sinsinwar, and V. Gupta. 2009. "Recent Developments in Groundnut Carbon Assimilation, Pathology, Molecular Biology." In *Crop Breeding and Biotechnology*, edited by C. P. Malik, C. Wadhwani, and B. Kaur, 161–191. Pointer Publishers.

Yang, J., A. K. Mattoo, Y. Liu, F. Zvomuya, and H. He. 2023. "Trade-Offs of Organic and Organic-Inorganic Fertilizer Combinations in Tomato Quality and Yield: A Global Meta-Analysis (1992–2021)." *European Journal of Agronomy* 151: 126985.

Zhang, K., Y. Y. Su, and L. Cai. 2013. "An Optimized Protocol of Single Spore Isolation for Fungi." *Cryptogamie, Mycologie* 34: 349–356.

Zhang, Y., H. Yang, D. Turra, et al. 2020. "The Genome of Opportunistic Fungal Pathogen *Fusarium oxysporum* Carries a Unique Set of Lineage-Specific Chromosomes." *Communications Biology* 3: 50.

Zhu, Z., and S. A. Miller. 2025. "Greenhouse Gas Emissions of Tomato Production and Supply: A Systematic Review." *Resources, Conservation and Recycling* 218: 108236.

Supporting Information

Additional supporting information can be found online in the Supporting Information section. **Table S1:** Details of the *Fusarium oxysporum* isolates collected from processing tomato fields in NSW and VIC, and reference isolates obtained from Queensland Plant Pathology Herbarium (BRIP). β-tubulin (*tub2*), calmodulin (*cmdA*), the second largest subunit of nuclear RNA polymerase II (*rpb2*) and translation elongation factor 1-α (*tef1-α*), were generated for all isolates. The unique sequence types (haplotypes) for each sequenced region and the four-locus haplotype for each isolate are shown.